

Application of the quantum spin glass theory to image restoration

Jun-ichi Inoue

*Complex Systems Engineering, Graduate School of Engineering,
Hokkaido University, N13-W8, Kita-ku, Sapporo, 060-8628, Japan*

(October 31, 2018)

Abstract

Quantum fluctuation is introduced into the Markov random fields (MRF's) model for image restoration in the context of Bayesian approach. We investigate the dependence of the quantum fluctuation on the quality of BW image restoration by making use of statistical mechanics. We find that the maximum posterior marginal (MPM) estimate based on the quantum fluctuation gives a fine restoration in comparison with the maximum a posterior (MAP) estimate or the thermal fluctuation based MPM estimate.

PACS numbers : 02.50.-r, 05.20.-y, 05.50.-q

I. INTRODUCTION

Recently, the problems of information science were investigated from statistical mechanical point of view. Among them, the image restoration is one of the most suitable subjects. In the standard approach to the image restoration, an estimate of the original image is given by maximizing a posterior probability distribution (the MAP estimate) [1]. In the context of statistical mechanics, this approach corresponds to finding the ground state configuration of the effective Hamiltonian for some spin system under the random fields. On the other hand, it is possible to construct another strategy to infer the original image using the thermal equilibrium state of the Hamiltonian. From the Bayesian statistical point of view, the *finite temperature restoration* coincides with maximizing a posterior marginal distribution (the MPM estimate [2,3]) and using this strategy, the error for each pixel may become smaller than that of the MAP estimate. As we use the average of each pixel (spin) over the Boltzmann-Gibbs distribution at a specific temperature, the thermal fluctuation should play an important role in the MPM estimate. Then, the temperature controls the shape of the distribution and if we choose the temperature appropriately, the sampling from the distribution generates the important configurations for a fine restoration. Besides this hill-climbing mechanism by the thermal fluctuation, we may use another type of fluctuation, namely, the quantum fluctuation which leads to quantum tunneling between the states. If we use the sampling from the Boltzmann-Gibbs distribution based on the quantum fluctuation, it may be possible to obtain much more effective configurations for a good restoration. The idea of the MRF's model using the quantum fluctuation was recently proposed by Tanaka and Horiguchi [4], however, they investigated the quantum fluctuation in the context of the optimization (the MAP estimate by the quantum fluctuation) and they used the ground state as the estimate of the original image. We would like to stress that we use the distribution based on the quantum fluctuation itself and the expectation value is used to infer the original image.

It is highly non-trivial problem to investigate whether the MPM estimate based on the quantum fluctuation becomes better than the MAP estimate or the thermal fluctuation based MPM estimate.

This is a basic concept of this paper. This paper is organized as follows. In the next Sec. II, we explain our model system and the basic idea of our method in detail. In Sec. II, we also introduce the criterion of the restoration, that is, the overlap between the original image and the result of the restoration. In Sec. III, we introduce the infinite range model in order to obtain analytical results on the performance of the restoration, and calculate the overlap explicitly. In Sec. IV, we show that quantum Monte Carlo simulations in 2-dimension support our analytical results. In Sec. V, we introduce the iterative algorithm which is derived by mean-field approximation and apply this algorithm to image restoration for standard pictures. The last Sec. VI is devoted to discussion about all results we obtain. In this section, we also mention the inequality which gives the upper bound of the overlap.

II. BASIC IDEA AND FORMULATION

Let us suppose that the original image is represented by a configuration of Ising spins $\{\xi\} \equiv \{\xi_i | \xi_i = \pm 1; i = 1, \dots, N\}$ with probability $P_s(\{\xi\})$. These images are sent through the noisy channel by the form of sequence $\{\xi\}$. Then, we regard the output of the sequence $\{\xi\}$ through the noisy channel as $\{\tau\}$. The output probability for the case of the binary symmetric channel (BSC) is specified by the following form;

$$P_{\text{out}}(\{\tau\} | \{\xi\}) = \frac{1}{(2\cosh\beta_\tau)^N} \exp\left(\beta_\tau \sum_i \tau_i \xi_i\right). \quad (1)$$

We easily understand the relevance of this expression for the BSC; Lets suppose that each pixel ξ_i changes its sign with probability p_τ and remains with $1 - p_\tau$ during the transmission, that is,

$$P(\tau_i = -\xi_i | \xi_i) = p_\tau \equiv \frac{e^{-\beta_\tau}}{2 \cosh \beta_\tau} \quad (2)$$

$$P(\tau_i = \xi_i | \xi_i) = 1 - p_\tau \equiv \frac{e^{\beta_\tau}}{2 \cosh \beta_\tau}. \quad (3)$$

We easily see that there is a simple relation between flip probability p_τ and inverse temperature β_τ as $\exp(2\beta_\tau) = (1 - p_\tau)/p_\tau$. This is reason why we refer to this type of noise as *binary symmetric* channel. Using the assumption that each pixel ξ_i in the original image $\{\xi\}$ is corrupted independently (so-called *memory-less channel*), namely, $P(\{\tau\} | \{\xi\}) = \prod_i P(\tau_i | \xi_i)$, we obtain Eq. (1). This BSC is simply extended to the following Gaussian channel (GC)

$$P_{\text{out}}(\{\tau\} | \{\xi\}) = \frac{1}{(\sqrt{2\pi}\tau)^N} \exp\left(-\frac{1}{2\tau^2} \sum_i (\tau_i - \tau_0 \xi_i)^2\right). \quad (4)$$

where τ is a standard deviation of observable (corrupted pixel) τ_i from scaled original pixel $\tau_0 \xi_i$.

Then, the posterior probability $P(\{\sigma\} | \{\tau\})$, which is the probability that the source sequence is $\{\sigma\}$ provided that the output is $\{\tau\}$, leads to

$$P(\{\sigma\} | \{\tau\}) = \frac{P(\{\tau\} | \{\sigma\}) P_m(\{\sigma\})}{\sum_\sigma P(\{\tau\} | \{\sigma\}) P_m(\{\sigma\})} \quad (5)$$

by the Bayes theorem. As we treat the BW image and the BSC (1), a likelihood $P(\{\tau\} | \{\xi\})$ is appropriately written by

$$P(\{\tau\} | \{\xi\}) \sim \exp\left(h \sum_i \tau_i \sigma_i\right). \quad (6)$$

$P_m(\{\sigma\})$ appearing in the Bayesian formula (5) is a model of the prior distribution $P_s(\{\xi\})$ and we usually use the following type;

$$P_m(\{\sigma\}) \sim \exp\left(\beta_m \sum_{\langle ij \rangle} \sigma_i \sigma_j\right) \quad (7)$$

where $\sum_{\langle ij \rangle} (\dots)$ means the sum with respect to the nearest neighboring pixels and β_m controls the smoothness of the picture according to our assumption. Substituting Eqs. (6) and (22) into Eq. (8), we obtain the posterior probability $P(\{\sigma\} | \{\tau\})$ explicitly;

$$P(\{\sigma\}|\{\tau\}) = \frac{\exp\left(\beta_m \sum_{\langle ij \rangle} \sigma_i \sigma_j + h \sum_i \tau_i \sigma_i\right)}{\sum_{\sigma} \exp\left(\beta_m \sum_{\langle ij \rangle} \sigma_i \sigma_j + h \sum_i \tau_i \sigma_i\right)}. \quad (8)$$

In the framework of the MAP estimate, we regard a configuration $\{\sigma\}$ which maximizes the posterior probability $P(\{\sigma\}|\{\tau\})$ as an estimate of the original image $\{\xi\}$. Obviously, this estimate $\{\sigma\}$ corresponds to the ground state of the following effective Hamiltonian (the random field Ising model)

$$\mathcal{H}_{\text{eff}} = -\beta_m \sum_{\langle ij \rangle} \sigma_i \sigma_j - h \sum_i \tau_i \sigma_i. \quad (9)$$

Therefore, in the limit of $\beta_m/h \rightarrow \infty$, we expect that the original image should be complete BLACK picture or complete WHITE picture, whereas in the limit of $\beta_m/h \rightarrow 0$, we assume that the original image should be identical to the observable $\{\tau\}$ itself.

On the other hand, in the framework of the MPM estimate, we maximize the following posterior marginal probability

$$P(\sigma_i|\{\tau\}) = \frac{\sum_{\sigma \neq \sigma_i} P(\{\tau\}|\{\sigma\}) P_m(\{\sigma\})}{\sum_{\sigma} P(\{\tau\}|\{\sigma\}) P_m(\{\sigma\})}. \quad (10)$$

As we treat the case of BW image, the estimate of the i -th pixel should be given as

$$\begin{aligned} & \text{sgn}\left(\sum_{\sigma_i=\pm 1} \sigma_i P(\sigma_i|\{\tau\})\right) \\ &= \text{sgn}\left(\frac{\sum_{\sigma} \sigma_i P(\{\tau\}|\{\sigma\}) P_m(\{\sigma\})}{\sum_{\sigma} P(\{\tau\}|\{\sigma\}) P_m(\{\sigma\})}\right) \\ & \equiv \text{sgn}(\langle \sigma_i \rangle_{h, \beta_m}) \end{aligned} \quad (11)$$

where $\langle \cdots \rangle_{h, \beta_m}$ means the average over the posterior probability Eq. (8). Consequently, our problem is reduced to that of statistical mechanics which is described by the effective Hamiltonian Eq. (9). As the Hamiltonian Eq. (9) has lots of local minima due to the quenched disorder $\{\tau\}$, in general, it is quite difficult to obtain the thermal equilibrium state which contributes to fine restoration without being trapped in a local minimum for a long time. In order to overcome this difficulty, we add the *quantum transverse field* [7]

$$-\Gamma \sum_i \hat{\sigma}_i^x \equiv \hat{\mathcal{H}}_1 \quad (12)$$

to the effective Hamiltonian (9) as *quantum fluctuation*. In this expression, $\hat{\sigma}_i^x$ means the x -component of the Pauli matrix and Γ controls the width of the quantum fluctuation. Intuitively, the term $\Gamma \hat{\sigma}_i^x$ is regarded as the *tunneling probability* between the eigenstates of the operator $\hat{\sigma}_i^z$ (z -component of the Pauli matrix), namely, $|\sigma_i^z = \pm 1\rangle$. The tunneling probability between the states $|\sigma_i^z = \pm 1\rangle$ leads to $|<\sigma_i^z = +1|\Gamma \hat{\sigma}_i^x|\sigma_i^z = -1>|^2 = \Gamma^2$. As the result, the term (12) generates the superposition of the states $|\sigma_i^z = +1\rangle$ (BLACK) and $|\sigma_i^z = -1\rangle$ (WHITE). Using this *fuzzy* representation for each pixel, we may construct the algorithm which is robust for the choice of the hyper-parameters, especially, for the edge parts of a given picture.

Our problem is now reduced to that of quantum statistical mechanics for the next effective Hamiltonian

$$\hat{\mathcal{H}}_{\text{eff}} = -h \sum_i \tau_i \hat{\sigma}_i^z - \beta_m \sum_{\langle ij \rangle} \hat{\sigma}_i^z \hat{\sigma}_j^z - \Gamma \sum_i \hat{\sigma}_i^x \equiv \hat{\mathcal{H}}_0 + \hat{\mathcal{H}}_1 \quad (13)$$

where we defined $\hat{\mathcal{H}}_1 \equiv \hat{\mathcal{H}}_{\text{eff}} - \hat{\mathcal{H}}_0$. Our main goal is to calculate the local magnetization $\langle \hat{\sigma}_i^z \rangle_{h, \beta_m, \Gamma}$ of the system described by the above Hamiltonian, that is to say,

$$\langle \hat{\sigma}_i^z \rangle_{h, \beta_m, \Gamma} \equiv \frac{\text{Tr}_\sigma \hat{\sigma}_i^z \exp(-\hat{\mathcal{H}}_{\text{eff}})}{\text{Tr}_\sigma \exp(-\hat{\mathcal{H}}_{\text{eff}})} \quad (14)$$

and regard the quantity $\text{sgn}(\langle \hat{\sigma}_i^z \rangle_{h, \beta_m, \Gamma})$ as an estimate of the original pixel ξ_i . Therefore, the averaged performance of our method is measured by the following *overlap* $M(h, \beta_m, \Gamma)$ as

$$M(h, \beta_m, \Gamma) = \text{Tr}_{\{\xi, \tau\}} P_s(\{\xi\}) P_{\text{out}}(\{\tau\} | \{\xi\}) \xi_i \text{sgn}(\langle \hat{\sigma}_i^z \rangle_{h, \beta_m, \Gamma}). \quad (15)$$

Then, our main interests are summarized as follows.

- Is it possible for us to use the quantum fluctuation in place of the thermal one ?
- Does there exist a specific choice of Γ which gives the optimal image restoration ?

Before we calculate the above overlap (15), we may add the *parity check term*, which was recently introduced by Nishimori and Wong [9], to the effective Hamiltonian (9). This parity check term is represented as $\beta_J \sum_{\langle ij \rangle} J_{ij} \hat{\sigma}_i^z \hat{\sigma}_j^z$, and we rewrite $\hat{\mathcal{H}}_0$ as

$$\hat{\mathcal{H}}_0 = -\beta_J \sum_{\langle ij \rangle} J_{ij} \hat{\sigma}_i^z \hat{\sigma}_j^z - \beta_m \sum_{\langle ij \rangle} \hat{\sigma}_i^z \hat{\sigma}_j^z - h \sum_i \tau_i \hat{\sigma}_i^z \quad (16)$$

where J_{ij} is the noisy version of the product of arbitrary two original pixels $\xi_i \xi_j$ and the output of this quantity through the noisy channel is given by

$$P_{\text{out}}(\{J\}|\{\xi\}) = \frac{1}{(2\cosh\beta_r)^{N_B}} \exp \left(\beta_r \sum_{\langle ij \rangle} J_{ij} \xi_i \xi_j \right) \quad (17)$$

for the BSC and

$$P_{\text{out}}(\{J\}|\{\xi\}) = \frac{1}{(\sqrt{2\pi}J)^{N_B}} \exp \left(-\frac{1}{2J^2} \sum_{\langle ij \rangle} (J_{ij} - J_0 \xi_i \xi_j)^2 \right) \quad (18)$$

for the GC, respectively. N_B is the number of the terms appearing in the sum in Eq. (17) or Eq. (18). Then, the effective Hamiltonian $\hat{\mathcal{H}}_{\text{eff}} = \hat{\mathcal{H}}_0 + \hat{\mathcal{H}}_1$ describes the thermodynamics of *quantum spin glass* [7,8] under random fields.

In the next section, we introduce the rather artificial model, namely, the infinite range model in which spins in the system (13) are fully connected.

III. THE INFINITE RANGE MODEL

In this section, we calculate the overlap (15) explicitly using the infinite range version of the effective Hamiltonian (13). We use the GC for the analysis of the infinite range model in this section and the BSC for the quantum Monte Carlo simulations in the next Sec. IV, respectively. However, these two channels can be treated by the following single form.

$$P_{\text{out}}(\{J\}|\{\tau\}) = \prod_{\langle ij \rangle} F_r(J_{ij}) \prod_{\langle ij \rangle} F_1(\tau_{ij}) \exp \left(\beta_r \sum_{\langle ij \rangle} J_{ij} \xi_i \xi_j + \beta_\tau \sum_i \tau_i \xi_i \right) \quad (19)$$

with

$$\begin{aligned} F_r(J_{ij}) &= \frac{1}{2\cosh\beta_r} \{ \delta(J_{ij} - 1) + \delta(J_{ij} + 1) \} \\ F_1(\tau_{ij}) &= \frac{1}{2\cosh\beta_\tau} \{ \delta(\tau_{ij} - 1) + \delta(\tau_{ij} + 1) \} \end{aligned} \quad (20)$$

for the BSC and with

$$\begin{aligned} F_r(J_{ij}) &= \frac{1}{\sqrt{2\pi J^2}} \exp\left(-\frac{1}{2J^2}(J_{ij}^2 + J_0^2)\right) \\ F_1(\tau_i) &= \frac{1}{\sqrt{2\pi\tau^2}} \exp\left(-\frac{1}{2\tau^2}(\tau_i^2 + \tau_0^2)\right), \end{aligned} \quad (21)$$

for the GC, and we set $\beta_J = J_0/J^2$, $\beta_\tau = \tau_0/\tau^2$.

As the original image, we use the ferro-magnetic snapshot from the distribution

$$P_s(\{\xi\}) = \frac{1}{Z(\beta_s)} \exp\left(\frac{\beta_s}{N} \sum_{ij} \xi_i \xi_j\right), \quad (22)$$

where $\sum_{ij}(\dots)$ means the sum over all possible combinations of (i, j) and we divided the argument of the exponential in Eq. (22) by N to take a proper thermo-dynamical limit as Hamiltonian should be of order N . For the same reason, we should re-scale the terms appearing in Eq. (13) as $\beta_J \sum_{ij} J_{ij} \hat{\sigma}_i^z \hat{\sigma}_j^z \rightarrow (\beta_J/N) \sum_{ij} J_{ij} \hat{\sigma}_i^z \hat{\sigma}_j^z$ and $\beta_m \sum_{ij} \hat{\sigma}_i^z \hat{\sigma}_j^z \rightarrow (\beta_m/N) \sum_{ij} \hat{\sigma}_i^z \hat{\sigma}_j^z$ when we treat the infinite range model.

It must be noted that $\hat{\mathcal{H}}_0$ and $\hat{\mathcal{H}}_1$ do not commute with each other and we use the following the Trotter decomposition [5]

$$Z = \lim_{P \rightarrow \infty} \text{Tr}_{\sigma^z} \left(e^{-\frac{\beta \mathcal{H}_0}{P}} e^{-\frac{\beta \mathcal{H}_1}{P}} \right)^P \quad (23)$$

to calculate the partition function explicitly. In this formula, \mathcal{H}_0 and \mathcal{H}_1 are eigenvalues of the operators $\hat{\mathcal{H}}_0$ and $\hat{\mathcal{H}}_1$ with respect to the following eigenvector

$$|\{\sigma_k^z\} > = \prod_{i=1}^N \bigotimes |\sigma_{ik}^z > \quad (k = 1, \dots, P) \quad (24)$$

with

$$\hat{\sigma}_{ik}^z |\sigma_{ik}^z > \equiv \sigma_{ik} |\sigma_{ik}^z >. \quad (25)$$

P means the Trotter number and we distinguish the different Trotter slices by the indices k .

Now we can calculate the partition function for the quantum spin system (16) in terms of the corresponding classical spin system whose dimension increases by 1. Using the Trotter formula (the path integral formula) and well-known replica method [6], namely,

$$[\ln \mathcal{Z}] = \lim_{n \rightarrow \infty} \frac{[\mathcal{Z}^n] - 1}{n}, \quad (26)$$

we can obtain the overlap as a function of the macroscopic parameters β_m and Γ by making use of the saddle point method. The bracket $[\dots]$ denotes the average over the distribution $P_s(\{\xi\})P_{\text{out}}(\{J\}, \{\tau\}|\{\xi\})$.

The standard replica calculations and saddle point method lead to the following coupled equations.

$$[\xi_i] = m_0 = \tanh(\beta_0 m_0) \quad (27)$$

$$[\langle \sigma_{iK}^\alpha \rangle_{h, \beta_m, \Gamma}] = m = \frac{\text{Tr}_\xi e^{\beta_s m_0 \xi}}{2 \cosh(\beta_s m_0)} \int_{-\infty}^{\infty} Du \Omega^{-1} \int_{-\infty}^{\infty} D\omega \Phi y^{-1} \sinhy \quad (28)$$

$$[\xi_i \langle \sigma_{iK}^\alpha \rangle_{h, \beta_m, \Gamma}] = t = \frac{\text{Tr}_\xi e^{\beta_s m_0 \xi}}{2 \cosh(\beta_s m_0)} \int_{-\infty}^{\infty} Du \Omega^{-1} \int_{-\infty}^{\infty} D\omega \xi \Phi y^{-1} \sinhy \quad (29)$$

$$[\langle (\sigma_{iK}^\alpha)^2 \rangle_{h, \beta_m, \Gamma}] = Q = \frac{\text{Tr}_\xi e^{\beta_s m_0 \xi}}{2 \cosh(\beta_s m_0)} \int_{-\infty}^{\infty} Du \left[\Omega^{-1} \int_{-\infty}^{\infty} D\omega \Phi y^{-1} \sinhy \right]^2 \quad (30)$$

$$\begin{aligned} [\langle \sigma_{iK}^\alpha \sigma_{iL}^\alpha \rangle_{h, \beta_m, \Gamma}] = S = & \frac{\text{Tr}_\xi e^{\beta_s m_0 \xi}}{2 \cosh(\beta_s m_0)} \int_{-\infty}^{\infty} Du \Omega^{-1} \left[\int_{-\infty}^{\infty} D\omega \Phi^2 y^{-2} \cosh y \right. \\ & \left. + \Gamma^2 \int_{-\infty}^{\infty} D\omega y^{-3} \sinhy \right], \end{aligned} \quad (31)$$

where $\langle \dots \rangle_{h, \beta_m, \Gamma}$ means the average by the posterior probability using the same way as Eq. (14). Du or Dy means Gaussian integral measure $Du \equiv du e^{-u^2/2}/\sqrt{2\pi}$. In order to obtain the above saddle point equations, we used the replica symmetric and the static approximation, that is,

$$t_K = t \quad (32)$$

$$S_\alpha(KL) = S(K \neq L), \quad 1(K = L) \quad (33)$$

$$Q_{\alpha\beta} = Q. \quad (34)$$

We also defined functions Φ , y and Ω as

$$\Phi \equiv u \sqrt{(\tau h)^2 + Q(J\beta_J)^2} + J\beta\omega \sqrt{S - Q} + (\tau_0 h + J_0 \beta_J t) \xi + \beta_m m \quad (35)$$

$$y \equiv \sqrt{\Phi^2 + \Gamma^2} \quad (36)$$

$$\Omega \equiv \int_{-\infty}^{\infty} D\omega \cosh y. \quad (37)$$

Then the overlap which is a measure of retrieval quality is calculated explicitly as

$$[\xi_i \operatorname{sgn}(\langle \sigma_{iK}^\alpha \rangle_{h, \beta_d, \Gamma})] = M = \frac{\operatorname{Tr}_\xi \xi e^{\beta_s m_0 \xi}}{2 \cosh(\beta_s m_0)} \int_{-\infty}^{\infty} Du \int_{-\infty}^{\infty} Dw \times \operatorname{sgn} \left[u \sqrt{(\tau h)^2 + Q(J\beta_J)^2} + (\tau_0 h + J_0 \beta_J t) \xi + \beta_m m + J \beta_J w \sqrt{S - Q} \right] \quad (38)$$

where the above overlap M depends on Γ through m (28).

We first consider the case of $\beta_J = 0$, that is to say, the conventional image restoration. We choose a snapshot from the distribution (22) at source temperature $T_s = 0.9$. According to Nishimori and Wong [9], we fix the ratio h/β_m and adjust $\beta_m (= 1/T_m)$ as a parameter for simulated annealing [10] and controls Γ as a quantum fluctuation. If we set $\Gamma = 0$, the lines of $M(T_m, \Gamma = 0)$ should be identical to the results by the *thermal* MPM estimate [9]. On the other hand, if we choose $T_m = 0$ and $\Gamma = 0$, the resultant line $M(T_m = 0, \Gamma)$ represents the performance of the *quantum* MAP estimate. We should draw attention to the fact that the quantum fluctuation vanishes at $\Gamma = 0$. In practical applications of the *quantum annealing* [12] based on quantum Monte Carlo simulations, we should reduce Γ from $\Gamma > 0$ to $\Gamma = 0$ during Monte Carlo updates. However, the resultant performance obtained here is calculated analytically provided that the system reaches its equilibrium state. Therefore, we can regard the result $M(T_m = 0, \Gamma = 0)$ as a performance when Γ is decreased slowly enough.

In FIG. 1, we set the ratio h/β_m to its optimal value $\beta_\tau/\beta_s = 0.9$ and plot the overlap $M(T_m, \Gamma)$ for the case of $\Gamma = 0, 0.5$ and $\Gamma = 1.0$. Obviously, for the case of $\Gamma = 0$, the maximum is obtained at a specific temperature $T_m = 0.9 (= T_s)$ [9]. However, if we add a finite quantum fluctuation, the optimal temperature T_m is shifted to the low temperature region.

In FIG. 2, we plot $M(T_m, \Gamma)$ for the case of $T_m = 0, 0.1, 0.9$ with the fixed optimal ratio $h/\beta_m = 0.9$. This figure shows that if we set the parameters h, β_m to their optimal value in the thermal MPM estimate, the quantum fluctuation added to the system destroys the recovered image (see the lines $M(T_m, \Gamma)$ for the case of $T_m = 0.9$). Therefore, we

may say that it is impossible to choose all parameters h, β_m and Γ so as to obtain the overlap which is larger than $M_{\max} \equiv M(T_m = 0.9, \Gamma = 0)$. This fact is also shown by 3-dimensional plot $M(T_m, \Gamma)$ in FIG. 3.

Although, we found that a finite Γ does not give the absolute maximum of the overlap, the *quantum* MPM estimate $M(T_m = 0, \Gamma > 0)$ has another kind of advantages. As FIG. 3 indicates, the overlap of the the quantum MPM estimate is almost flat in comparison with $M(T_m = 0.1, \Gamma > 0)$ or $M(T_m = 0.9, \Gamma > 0)$. This is a desirable property from practical point of view. This is because the estimation of the hyper-parameters is one of the crucial problems to infer the original image, and in general, it is difficult to estimate them beforehand. Therefore, this robustness for hyper-parameter selection is a desirable property. We also see this property in FIG. 3.

As we already mentioned, the overlap at $T_m = 0$ and $\Gamma = 0$ corresponds to the result which is obtained by quantum annealing [12], that is to say, the quantum MAP estimate. We see that the result of the quantum MPM estimate is slightly better than that of the quantum MAP estimate.

We next show the effect of the parity check term. In FIG. 4, we set $T_m = T_s = 0.9, h = 1.0$ and $J_0 = J = 1.0$ and plot the overlap as a function of β_J for several values of Γ . We see that the performance of the restoration is improved by introducing the parity check term which has much information about the local structure of the original image.

In the next section, we check the usefulness of this method in terms of quantum Monte Carlo simulation.

IV. QUANTUM MONTE CARLO SIMULATION

In this section, Monte Carlo simulations in realistic 2-dimension are carried out in order to check the practical usefulness of our method. We use the *standard pictures* which are provided on the web site [11] as the original image, instead of the Ising snapshots. In order to sampling the important points which contribute to the local magnetization

$\langle \hat{\sigma}_i^z \rangle$, we use the quantum Monte Carlo method which was proposed by Suzuki [5]. As we mentioned in the previous sections, we can treat the d -dimensional quantum system as $(d + 1)$ -dimensional classical system by the Trotter decomposition [5]. In this sense, the transition probability of the Metropolis algorithm leads to

$$P(\boldsymbol{\sigma} \rightarrow \boldsymbol{\sigma}') = \min \left[1, \exp(-(E(\boldsymbol{\sigma}') - E(\boldsymbol{\sigma}))) \right] \quad (39)$$

where $E(\boldsymbol{\sigma})$ is energy of the classical spin system in $(d + 1)$ -dimension (in the present case, $(2 + 1) = 3$ -dimension) as follows.

$$E(\boldsymbol{\sigma}) \equiv -\frac{\beta_m}{P} \sum_{ijk} [\sigma_{i,j,k} \sigma_{i+1,j,k} + \sigma_{i,j,k} \sigma_{i-1,j,k} + \sigma_{i,j,k} \sigma_{i,j+1,k} + \sigma_{i,j,k} \sigma_{i,j-1,k}] - \frac{h}{P} \sum_{ijk} \tau_{i,j} \sigma_{i,j,k} - B \sum_{ijk} \sigma_{i,j,k} \sigma_{i,j,k+1} \quad (40)$$

where we defined $B \equiv \ln \cosh(\Gamma/P)$. The transition probability Eq. (39) with Eq. (40) generates the Boltzmann-Gibbs distribution asymptotically and using the importance sampling from the distribution, we can calculate the expectation value of the i -th spin $\hat{\sigma}_i^z$, namely, $\langle \hat{\sigma}_i^z \rangle_{h,\beta_m,\Gamma}$, and using this result, we obtain an estimate of the i -th pixel of the original image as $\text{sgn}(\langle \hat{\sigma}_i^z \rangle_{h,\beta_m,\Gamma})$. We show the results in FIG.s 5 and 6. From these Figures, we see that there exists the optimal value of the transverse field Γ . In FIG.s 7 and 8, we display the results by quantum Monte Carlo simulations when we add the parity check term for the parameter sets $\Gamma = 2.0$, $h = 1.0$ and $\beta_m = 0.5$. We see that the resultant pictures using the parity check term are almost perfect (see $\beta_J = 1.0$ and 1.5).

V. MEAN-FIELD ALGORITHM

In the previous sections, we see that the quantum fluctuation works effectively on image restoration problems in the sense that the quantum fluctuation suppress the error of the hyper-parameter's estimation in the Markov random fields model. In addition, by making use of the quantum Monte Carlo simulations, we could apply it to the image restoration of the 2-dimensional standard pictures. However, in order to carry out the

simulations, it takes quite long time to obtain the average $\langle \hat{\sigma}_i^z \rangle_{h,\beta_m,\Gamma}$ and it is not suitable for practical situations.

In this section, in order to overcome this computational time intractability, we derive the iterative algorithm based on the mean-field approximation. This algorithm shows fast convergence to the approximate solution.

Within the mean-field approximation, we rewrite the density matrix $\hat{\rho} = e^{-\hat{\mathcal{H}}_{\text{eff}}}/\mathcal{Z}$ for 2-dimensional version of the effective Hamiltonian $\hat{\mathcal{H}}_{\text{eff}}$ as

$$\hat{\rho} \simeq \prod_{ij} \bigotimes \hat{\rho}_{ij}, \quad (41)$$

where we defined $\hat{\rho}_{ij}$ as

$$\hat{\rho}_{ij} = \sum_{n=1}^2 |\sigma_{ij}(n) > e^{-\lambda_{ij}(n)} \langle \sigma_{ij}(n)| \quad (42)$$

with

$$\mathcal{Z}_{ij} = e^{-\lambda_{ij}(1)} + e^{-\lambda_{ij}(2)}. \quad (43)$$

In the above expressions, $\lambda_{ij}(n)$, $n = 1, 2$ means eigenvalues of the 2×2 matrix $\hat{\mathbf{H}}_{ij}$ ($[\hat{\mathbf{H}}_{ij}]_{11} = H_{ij}^{(+)}$, $[\hat{\mathbf{H}}_{ij}]_{22} = H_{ij}^{(-)}$, $[\hat{\mathbf{H}}_{ij}]_{12} = [\hat{\mathbf{H}}_{ij}]_{21} = -\Gamma$) and $H_{ij}^{(\pm)}$ is defined by

$$\begin{aligned} H_{ij}^{(+)} &= -(\tau_{ij} + Jm_{i+1,j}^{(t)} + Jm_{i-1,j}^{(t)} + Jm_{i,j+1}^{(t)} + Jm_{i,j-1}^{(t)}) \\ &= -H_{ij}^{(-)} \equiv \alpha, \end{aligned} \quad (44)$$

$$J \equiv \frac{\beta_m}{h}. \quad (45)$$

Using this decoupled density matrix, the local magnetization at a site (i, j) , namely, $m_{ij}^{(t+1)}$ leads to

$$\begin{aligned} m_{ij}^{(t+1)} &= \text{Tr}[\sigma_{ij}^z \hat{\rho}_{ij}] \\ &= \frac{e^{\sqrt{\alpha^2 + \Gamma^2}}}{2\cosh(\sqrt{\alpha^2 + \Gamma^2})} \left[\frac{(\alpha + \sqrt{\alpha^2 + \Gamma^2})^2 - \Gamma^2}{(\alpha + \sqrt{\alpha^2 + \Gamma^2})^2 + \Gamma^2} \right] \\ &+ \frac{e^{-\sqrt{\alpha^2 + \Gamma^2}}}{2\cosh(\sqrt{\alpha^2 + \Gamma^2})} \left[\frac{(\alpha - \sqrt{\alpha^2 + \Gamma^2})^2 - \Gamma^2}{(\alpha - \sqrt{\alpha^2 + \Gamma^2})^2 + \Gamma^2} \right]. \end{aligned} \quad (46)$$

For this local magnetization (46), the estimate of the pixel ξ_{ij} is obtained as $\text{sgn}[m_{ij}]$.

We solve the mean-field equations (46) with respect to m_{ij} until the condition

$$\varepsilon_{ij} \equiv |m_{ij}^{(t+1)} - m_{ij}^{(t)}| < 10^{-5} \quad (47)$$

holds for all pixels $\{i, j\}$. We show its performance in FIG. 9 and TABLE I. From TABLE I, we see that if we introduce appropriate quantum fluctuation, the performance is remarkably improved, and in addition, the speed of the convergence becomes much faster. However, if we add the quantum fluctuation too much, the fluctuation destroys the recovered image. We also see that the optimal value of Γ exists around $\Gamma \sim 1.6$.

VI. SUMMARY AND DISCUSSION

In this paper, we investigated to what extent the quantum fluctuation works effectively on image restoration. For this purpose, we introduced an analytically solvable model, that is, the infinite range version of the MRF's model. We applied the technique of statistical mechanics to this model and derived the overlap explicitly. We found that the quantum fluctuation improves the quality of the image restoration dramatically at a low temperature region. In this sense, the error of the estimation for the hyper-parameters β_m, h can be suppressed by the quantum fluctuation.

However, we also found that the maximum value of the overlap $M_{\max}^{(\text{quantum})}$ never exceeds that of the classical Ising case $M_{\max}^{(\text{thermal})}$. We may show this fact by the following arguments; First of all, the upper bound of the overlap for the classical system is given by setting $h = \beta_\tau, P_s = P_m$, that is,

$$\begin{aligned} M_{\max}^{(\text{thermal})}(\beta_\tau, P_s) &= \text{Tr}_{\{\tau, \xi\}} \xi_i e^{\beta_\tau \sum_i \tau_i \xi_i} P(\{\xi\}) \text{sgn}[\text{Tr}_\sigma \sigma_i e^{\beta_\tau \sum_i \tau_i \sigma_i} P_m(\{\sigma\})] \\ &= \text{Tr}_{\{\tau, \xi\}} \xi_i e^{\beta_\tau \sum_i \tau_i \xi_i} P(\{\xi\}) \cdot \frac{\text{Tr}_\sigma \sigma_i e^{\beta_\tau \sum_i \tau_i \sigma_i} P_m(\{\sigma\})}{|\text{Tr}_\sigma \sigma_i e^{\beta_\tau \sum_i \tau_i \sigma_i} P_m(\{\sigma\})|} \\ &= \text{Tr}_\tau |\text{Tr}_\sigma \sigma_i e^{\beta_\tau \sum_i \tau_i \sigma_i} P_m(\{\sigma\})|. \end{aligned} \quad (48)$$

For the quantum system, the overlap is bounded by this maximum value $M_{\max}^{(\text{classical})}$ as

$$\begin{aligned}
M^{(\text{quantum})}(h, P_m, \Gamma) &= \text{Tr}_{\{\tau, \xi\}} \xi_i e^{\beta_\tau \sum_i \tau_i \xi_i} P(\{\xi\}) \text{sgn}[\text{Tr}_{\hat{\sigma}} \hat{\sigma}_i^z e^{h \sum_i \tau_i \hat{\sigma}_i^z + \Gamma \sum_i \hat{\sigma}_i^x} P_m(\hat{\sigma}^z)] \\
&\leq |\text{Tr}_{\{\tau, \xi\}} \xi_i e^{\beta_\tau \sum_i \tau_i \xi_i} P(\{\xi\}) \text{sgn}[\text{Tr}_{\hat{\sigma}} \hat{\sigma}_i^z e^{h \sum_i \tau_i \hat{\sigma}_i^z + \Gamma \sum_i \hat{\sigma}_i^x} P_m(\{\hat{\sigma}_i^z\})]| \\
&= \text{Tr}_\tau |\text{Tr}_\xi \xi_i e^{\beta_\tau \sum_i \tau_i \xi_i} P(\{\xi\})| = M_{\max}^{(\text{thermal})}.
\end{aligned} \tag{49}$$

We can see this inequality more directly as follows.

$$\begin{aligned}
\text{Tr}_\tau |\text{Tr}_\xi \xi_i e^{\beta_\tau \sum_i \tau_i \xi_i} P(\{\xi\})| &\geq \text{Tr}_{\{\tau, \xi\}} \xi_i e^{\beta_\tau \sum_i \tau_i \xi_i} P(\{\xi\}) \cdot \frac{\text{Tr}_{\hat{\sigma}} \hat{\sigma}_i^z e^{h \sum_i \tau_i \hat{\sigma}_i^z + \Gamma \sum_i \hat{\sigma}_i^x} P_m(\{\hat{\sigma}^z\})}{|\text{Tr}_{\hat{\sigma}} \hat{\sigma}_i^z e^{h \sum_i \tau_i \hat{\sigma}_i^z + \Gamma \sum_i \hat{\sigma}_i^x} P_m(\{\hat{\sigma}^z\})|} \\
&= \text{Tr}_{\{\tau, \xi\}} \xi_i e^{\beta_\tau \sum_i \tau_i \xi_i} P(\{\xi\}) \text{sgn}[\text{Tr}_{\hat{\sigma}} \hat{\sigma}_i^z e^{h \sum_i \tau_i \hat{\sigma}_i^z + \Gamma \sum_i \hat{\sigma}_i^x} P_m(\{\hat{\sigma}^z\})] \\
&= M^{(\text{quantum})}(h, P_m, \Gamma),
\end{aligned} \tag{50}$$

where the identity $\text{sgn}(x) = x/|x|$ was used. We should notice that in the left hand side of the above inequality (50), the arguments of the trace w. r. t. τ always take positive values, while in the right hand side, they can be negative.

In order to check the usefulness of the method, we carried out quantum Monte Carlo simulations in realistic 2-dimension. We found that the results by the simulation support qualitative behavior of the analytical expressions for overlap.

We introduced the iterative algorithm in terms of the mean-field approximation and applied it to image restoration of the standard pictures. We found that the quantum fluctuation suppress the error of the hyper-parameter estimation. In addition, we found that the speed of the convergence to the solution is accelerated by the quantum fluctuation.

From all results obtained in this paper, we concluded that the quantum fluctuation turns out to enhance tolerance against uncertainties in hyper-parameter estimation. However, if much higher quantities of restoration are required, we must estimate those parameters using some methods. One of the strategies for this purpose is selecting the parameters β_m, h and Γ which maximize a *marginal likelihood*. By making use of the infinite range model, the usefulness of this method can be evaluated. The details of the analysis will be reported in forth coming paper.

Of course, the application of this strategy to the restoration of gray-scaled image [13,14] will be considered as an important future problem.

The author acknowledges H. Nishimori for fruitful discussions and useful comments. He also thanks K. Tanaka for kind tutorial on the theory of image restoration and drawing his attention to reference [4]. He acknowledges D. Bolle', A. C. C. Coolen, D. M. Carlucci, T. Horiguchi, P. Sollich and K. Y. M. Wong for valuable discussions. The author thanks Department of Physics, Tokyo Institute of Technology and Department of Mathematics, Kings College, University of London for hospitality.

This work was partially supported by the Ministry of Education, Science, Sports and Culture, Grant-in-Aid for Encouragement of Young Scientists, No. 11740225, 1999-2000 and also supported by the collaboration program between Royal Society and Japanese Physical Society.

REFERENCES

- [1] S. Geman and D. Geman, IEEE Trans., **PAMI** **6**, 721 (1984).
- [2] J. Marroquin, S. Mitter and T. Poggio, J. American Stat. Assoc., **82** 76, (1987).
- [3] J. M. Pryce and A. D. Bruce, J. Phys. A: Math. Gen. **28**, 511 (1995).
- [4] K. Tanaka and T. Horiguchi, The Transactions on The Institute of Electronics, Information and Communication Engineers **J80-A-12**, 2117 (1997) (in Japanese).
- [5] M. Suzuki, Prog. of Theor. Phys. **56** 1454 (1976).
- [6] D. Sherrington and S. Kirkpatrick, Phys. Rev. Lett. **35**, 1792 (1975).
- [7] K. Chakrabarti, A. Dutta and D. Sen, *Quantum Ising Phases and Transitions in Transverse Ising Models*, Lecture Note in Physics **41**, Springer (1996).
- [8] A. J. Bray and M. A. Moore, J. Phys. C **13**, L655 (1985).
- [9] H. Nishimori and K. Y. M. Wong, Phys. Rev. E **60** 132 (1999).
- [10] S. Kirkpatrick, C. D. Gelatt Jr. and M. D. Vecchi, Science **220** (1983).
- [11] The standard pictures which are used in this paper are available at
<ftp://ftp.lab1.kuis.kyoto-u.ac.jp/pub/sidba/>.
- [12] T. Kadowaki and H. Nishimori, Phys. Rev. E **58** 5355 (1998).
- [13] D. M. Carlucci and J. Inoue, Phys. Rev. E **60** 2547 (1999).
- [14] J. Inoue and D. M. Carlucci, Submitted to Phys. Rev. E (2000).

FIGURES

FIG. 1. The overlap M as a function of T_m for several values of Γ . We set the system parameters as $T_s = 0.9, \tau_0 = \tau = 1.0$ and $h/\beta_m = 0.9 = \beta_\tau/\beta_s$. For $\Gamma = 0$ case, the optimal temperature T_m coincides with the source temperature $T_s = 0.9$. As the quantum fluctuation Γ increases, the optimal temperature is shifted to a low temperature region. However, the maximum value of the overlap does not change.

FIG. 2. The overlap M as a function of Γ for several values of T_m . We set the system parameters as $T_s = 0.9, \tau_0 = \tau = 1.0$ and $h/\beta_m = 0.9 = \beta_\tau/\beta_s$. The overlap at $T_m = 0$ and $\Gamma = 0$ corresponds to the result by quantum annealing. The quantum MPM estimate works effectively at a low temperature region and the results are robust for the choice of Γ .

FIG. 3. The overlap M as a function of the quantum fluctuation Γ and temperature T_m .

FIG. 4. The overlap M as a function of β_J for several values of Γ . We set the system parameters $T_m = T_s = 0.9, \tau = \tau_0 = 1.0, J = J_0 = 1.0$ and $h/\beta_m = 0.9 = \beta_\tau/\beta_s$. For the case of $\Gamma = 0$, the optimal β_J is naturally identical to $J_0/J^2 = 1.0$. As the quantum fluctuation Γ increases, the overlap M decreases because the quantum fluctuation destroys the recovered image.

FIG. 5. The results by quantum Monte Carlo simulations for standard picture (A Japanese *Kanji* stamp for the name of *suzuki* which is the most popular name in Japan. The size is 50×50). From the upper left to the lower right, the original picture, the damaged picture, the results of $\Gamma = 0.2, 1.0, 1.7, 1.9, 2.1$ and 2.7 are displayed. The noise rate is 10% (The overlap between the original picture and the damaged one is 0.9).

FIG. 6. The overlap M as a function of the quantum fluctuation Γ for the standard picture in FIG. 5. We set $\beta_m = 0.5, h = 1.0$ and $P = 50$. The error-bars are calculated by averaging over five independent runs.

FIG. 7. The results by quantum Monte Carlo simulations including the parity check term.

We fixed $\Gamma = 2.0$, $h = 1.0$ and $\beta_m = 0.5$. From the upper left to the lower right, the original picture, the damaged picture, the results of $\beta_J = 0.01, 0.5, 1.0$ and 1.5 are shown. The noise rate is 10% (The overlap between the original picture and the damaged one is 0.9).

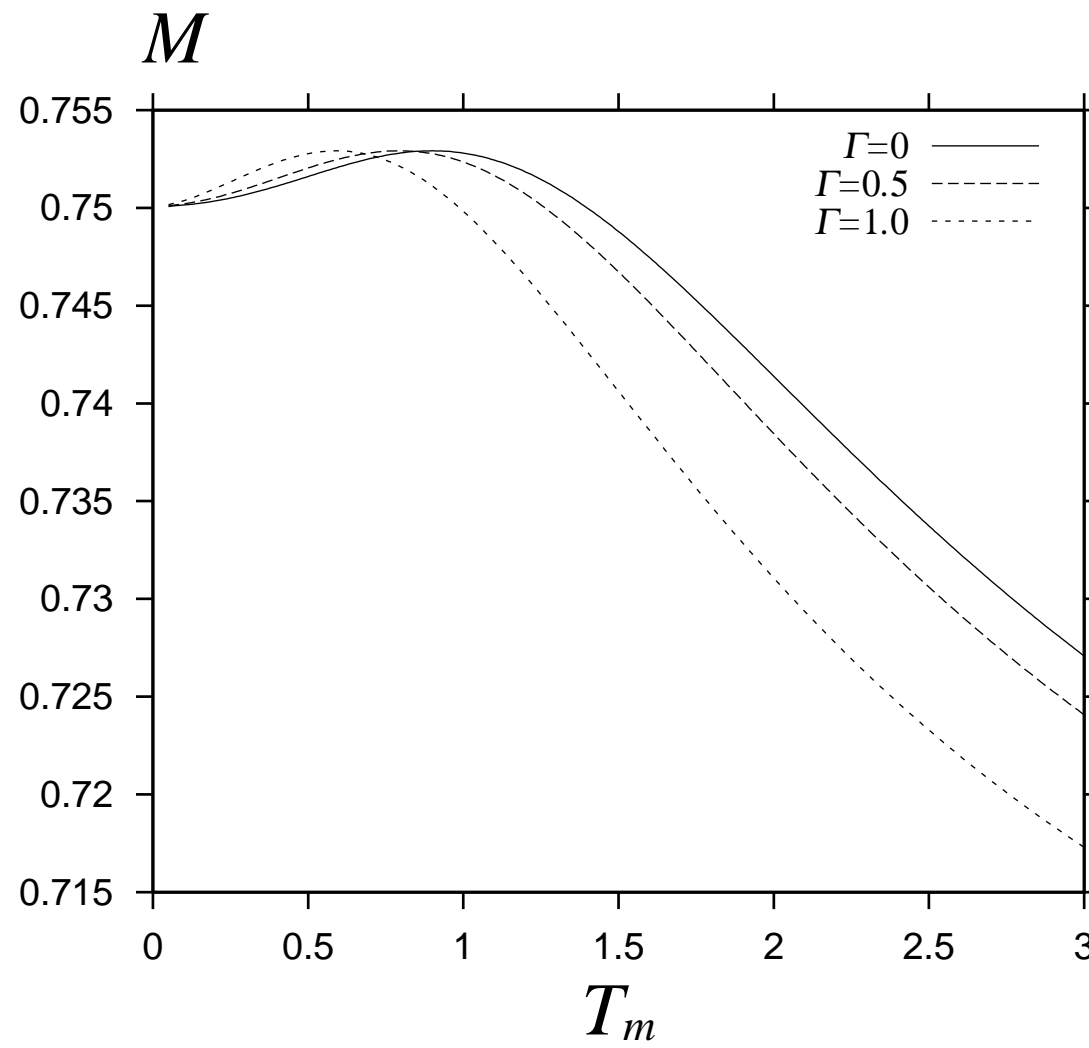
FIG. 8. β_J -dependence of the overlap M calculated by quantum Monte Carlo simulations for standard picture in FIG. 6. We set $\beta_m = 0.5$, $h = 1.0$ and $\Gamma = 2.0$. The error-bars are calculated by five independent runs.

FIG. 9. The restored pictures (Their size are 50×50) by quantum iterative algorithm for several values of Γ . From the upper left to the lower right, the original image, the corrupted image, the results of $\Gamma = 0.001, 0.8, 1.2, 1.6, 2.0$ and $\Gamma = 3.0$. The noise rate is 20% (The overlap between the original picture and the damaged one is 0.8).

TABLES

TABLE I. The overlap M calculated by the quantum iterative algorithm for several values of Γ . The restored pictures are shown in FIG. 9. The iteration times are also listed. We set $T = 1, J = 0.5$.

J. INOUE
FIG. 1

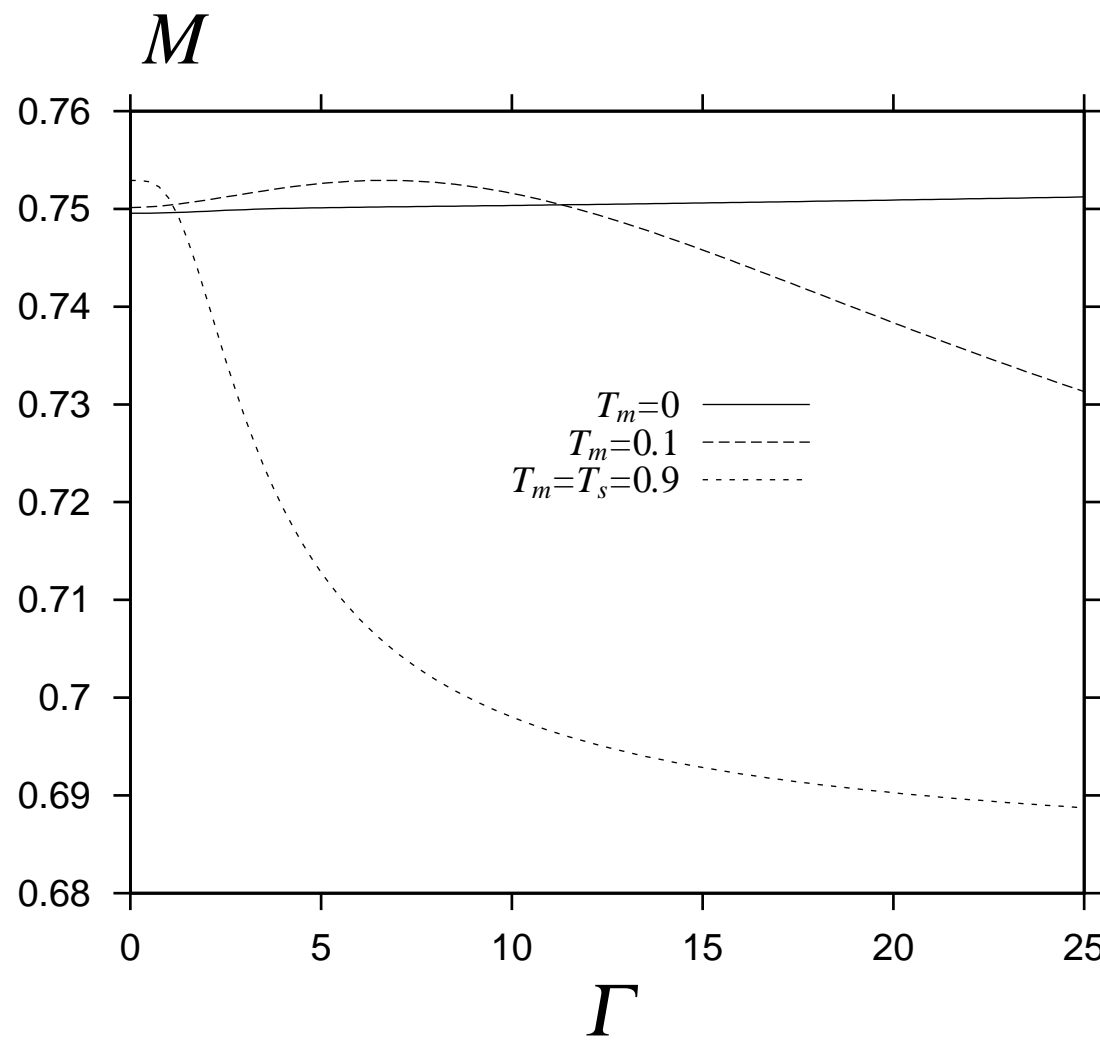


Γ	M	Iteration times
0.001000	0.919200	21
0.800000	0.921600	22
1.200000	0.927200	8
1.600000	0.932800	4
2.400000	0.900800	2
3.000000	0.840000	4

TABLE I
J. INOUE

J. INOUE

FIG. 2



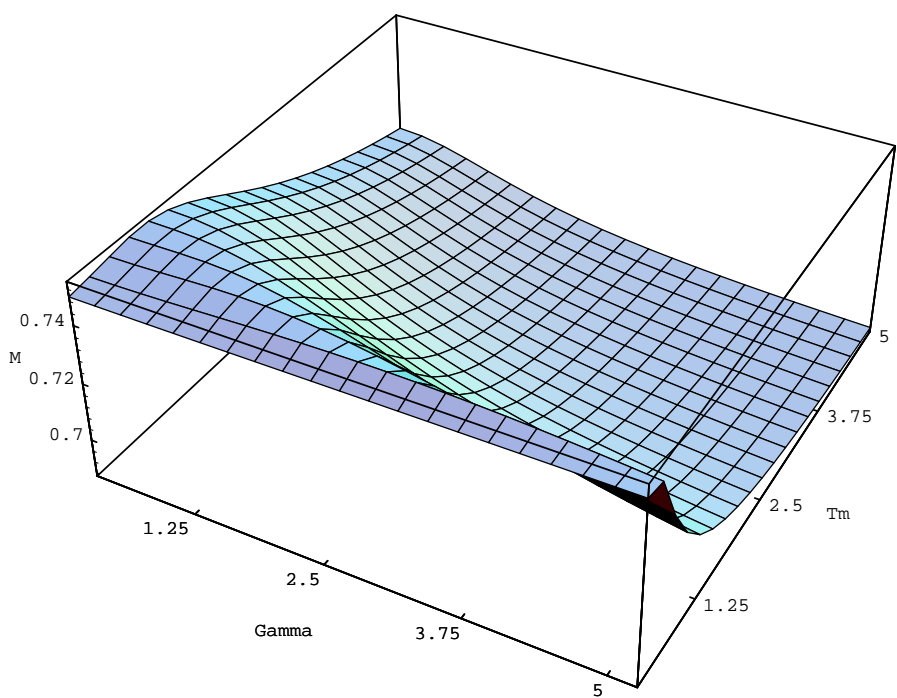
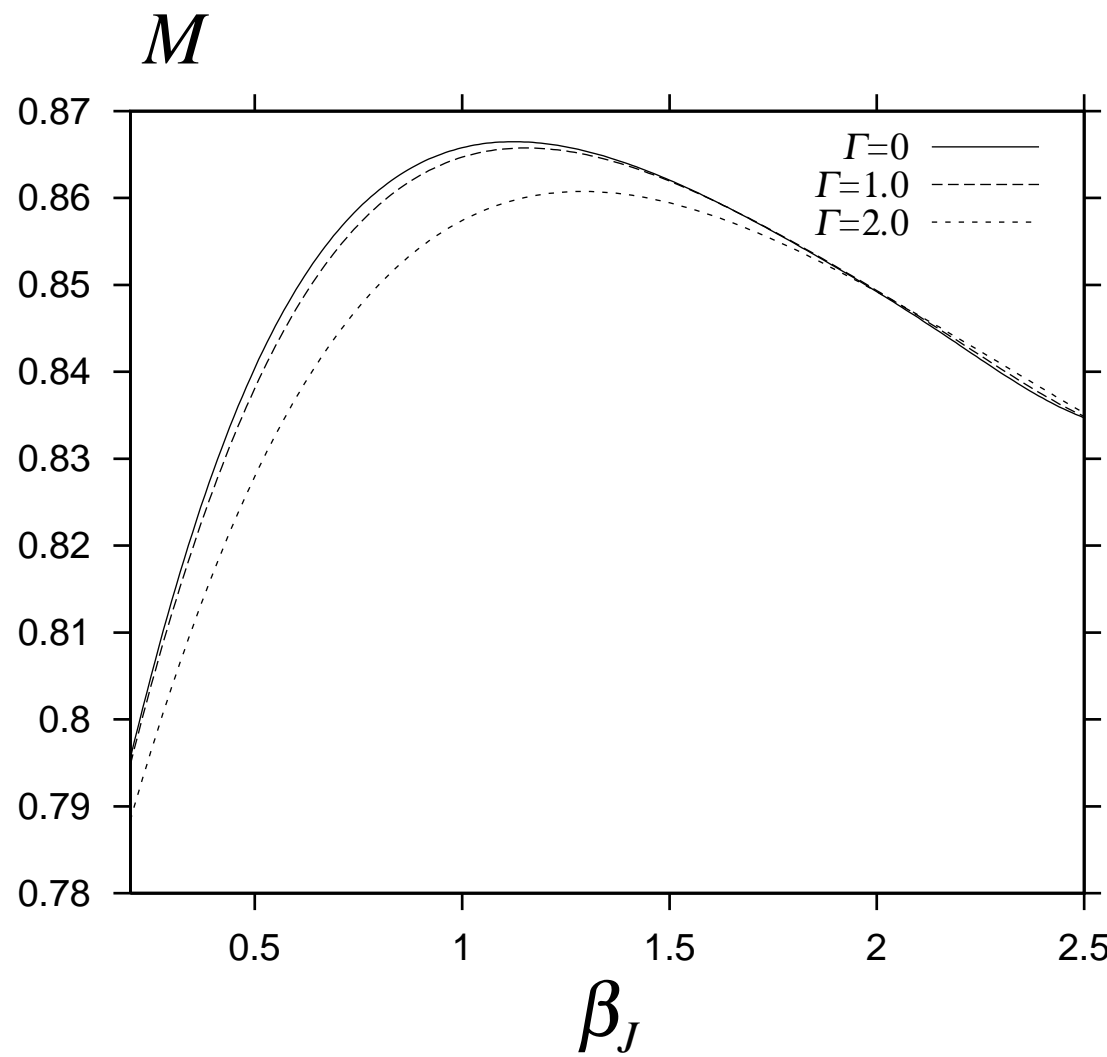


FIG. 3
J. INOUE

J. INOUE
FIG. 4



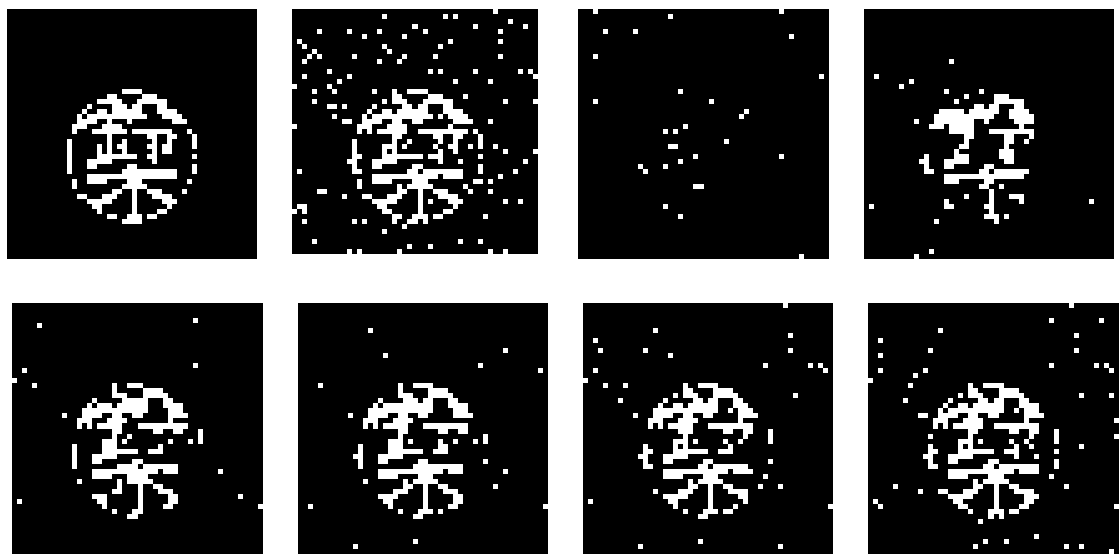
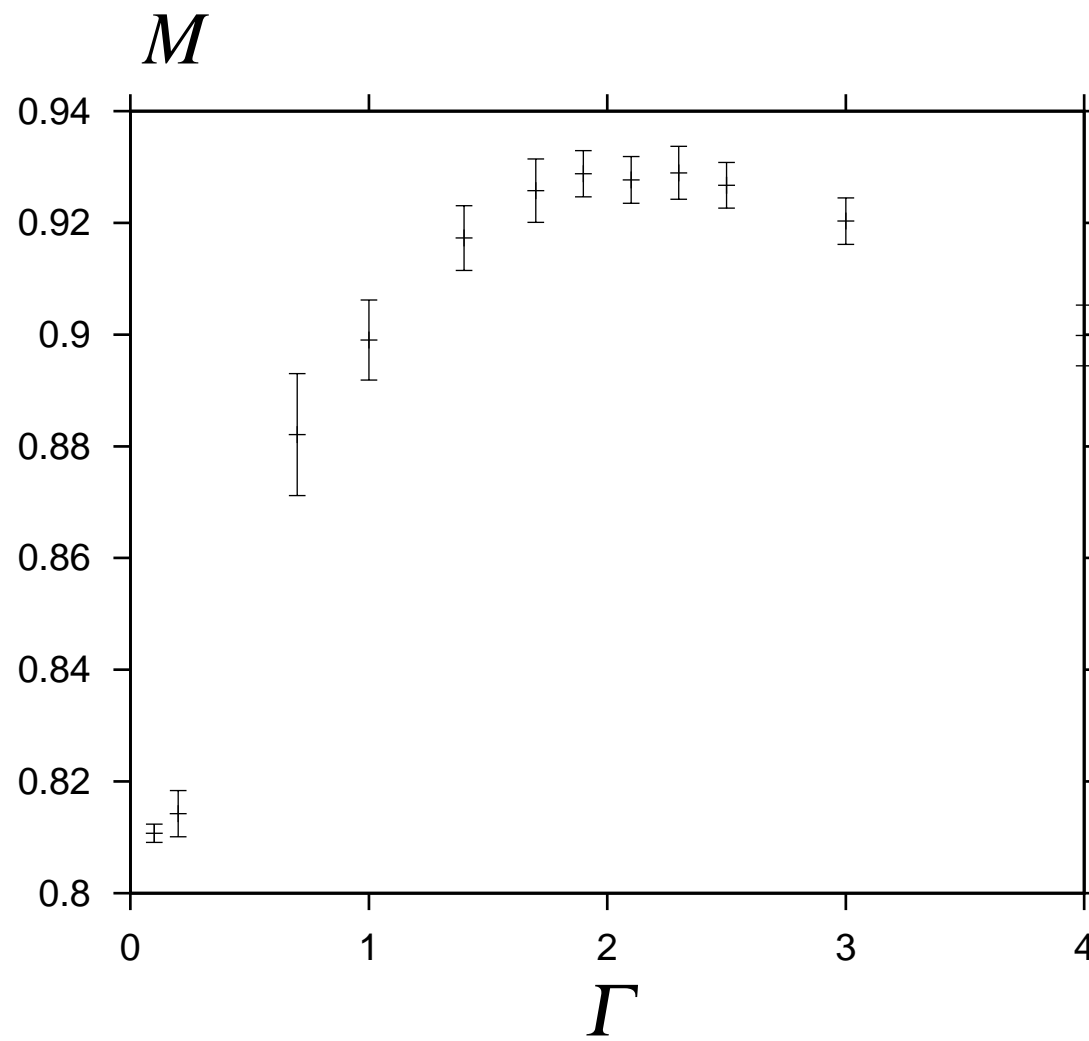


FIG. 5

J. INOUE

J. INOUE

FIG. 6



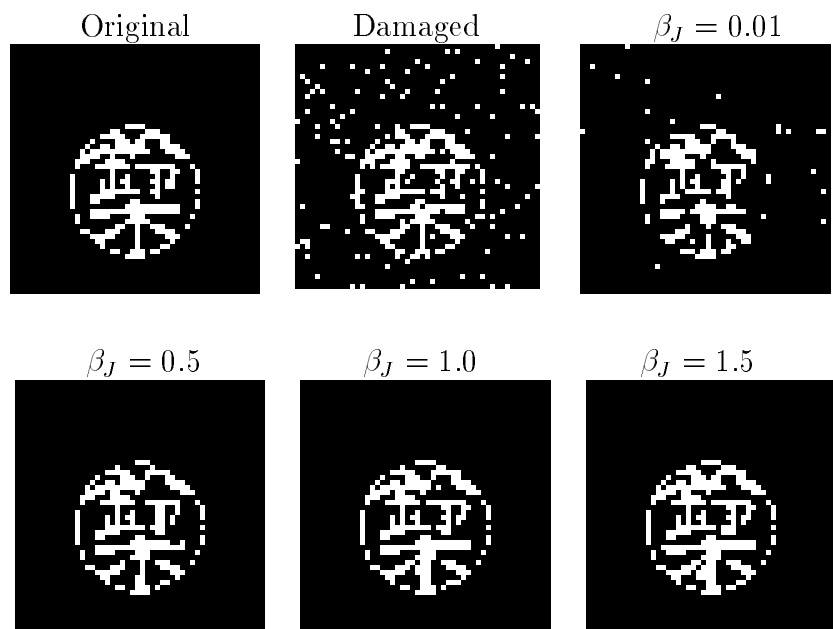
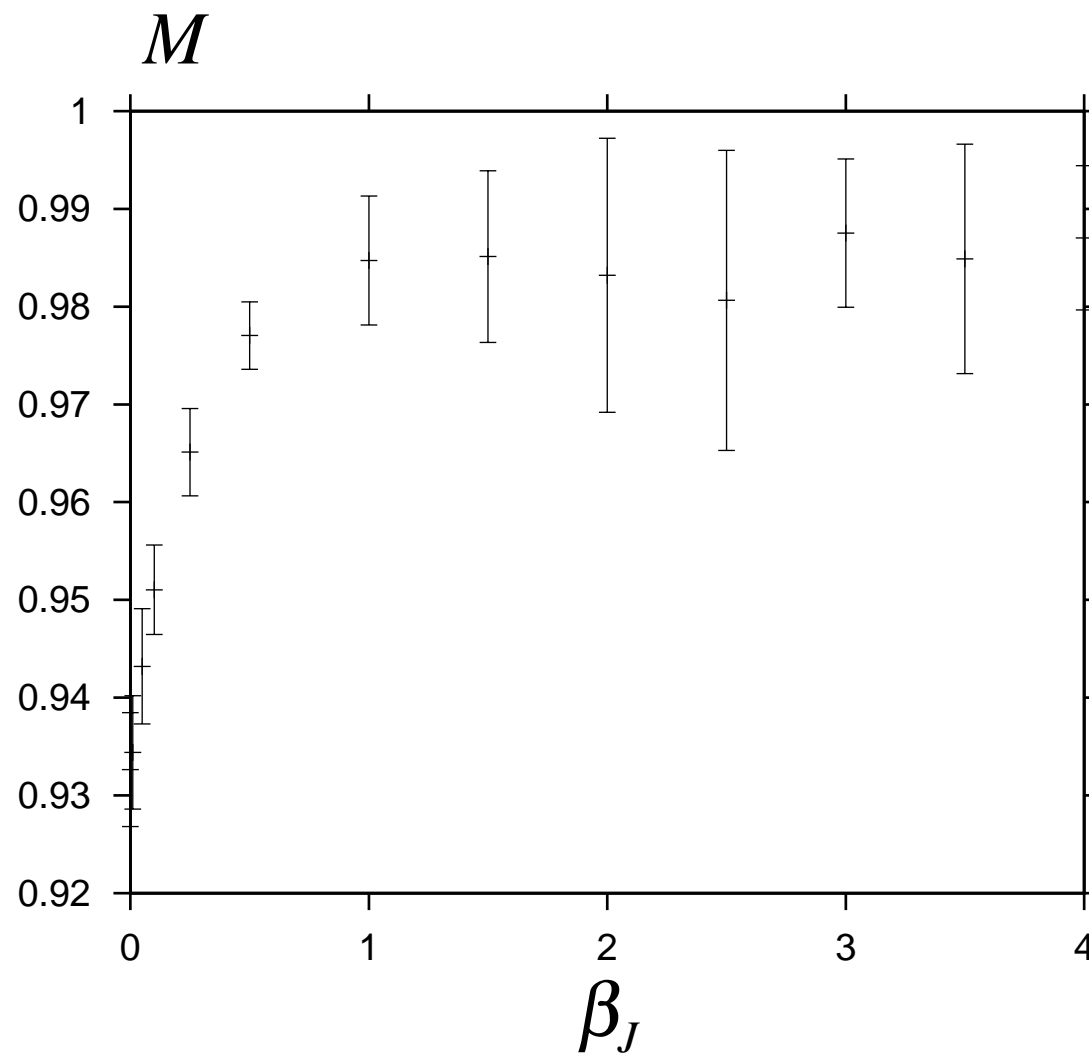


FIG. 7

J. INOUE

J. INOUE

FIG. 8



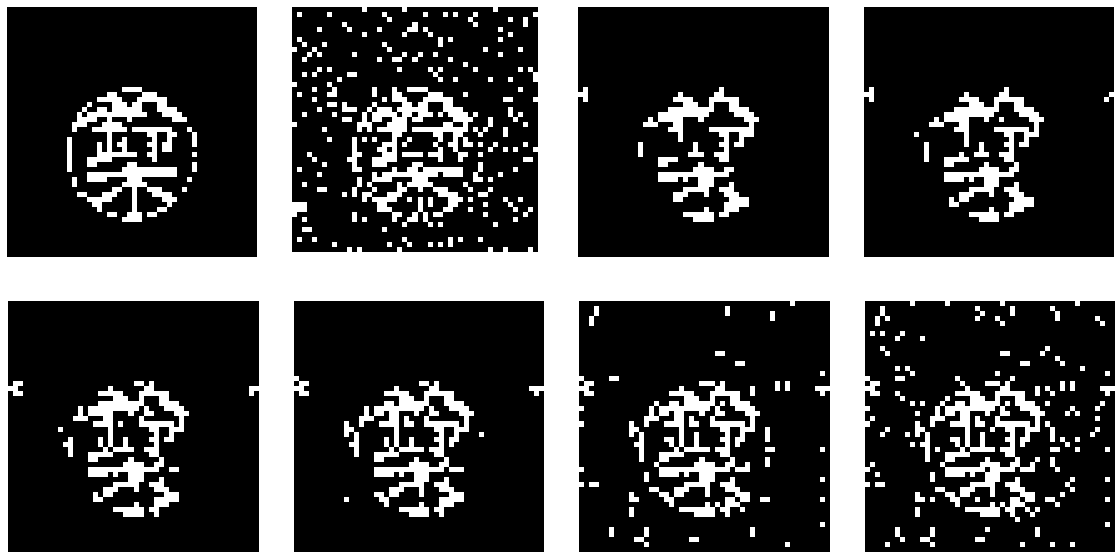


FIG. 9

J. INOUE